Development of distant metastases is the final stage of solid cancer progression and is responsible for the majority of cancer-related deaths. Distant metastatic spread has been considered to be a late process in malignant progression, but a recent study suggests that dissemination of primary cancer cells to distant sites might actually be an early event.[21] Disseminated tumor cells can be detected at early stages of tumor progression in lymph nodes, peripheral blood, and in bone marrow (BM) of cancer patients.[22,23] BM may be an important reservoir of tumor cells, from which they recirculate into distant organs such as liver or lungs. Furthermore, recent studies in vivo by Kaplan et al. and Gal et al. revealed that BM-derived cells are required for metastasis.[24,25] Indeed, in a large scale study of gastric cancer cases, we found that the simultaneous expression of epithelial markers (*CEA*, *CK-7*, and *CK-19*) and high levels of *VEGFR-1* expression in BM were significantly associated with hematogeneous metastases.[26]

The present study was designed to examine the clinical magnitude of *VIM* expression in BM and its relation to the progression of gastric cancer. The clinical findings suggest that *VIM* overexpression originates in epithelial cancer cells after the mesenchymal transition. Therefore, we first examined and determined the clinical significance of *VIM* mRNA expression in BM from gastric cancer patients, assessing both isolated tumor cells as well as adjacent host progenitor cells. Second, to provide explanations for clinical findings, we asked whether *VIM* expression was induced in gastric cancer cells by transforming growth factor-β1 (TGF-β1) or hypoxic treatments, both of which are recognized as important inducers of EMT.[10,27] Finally, to determine whether *VIM* expression provides cancer cells the ability to invade tumor vessels and to metastasize to BM, we examined the expression of VIM protein immunohistochemically in poorly differentiated stomach adenocarcinomas including 2 cases of gastric cancer with rhabdoid features.

MATERIALS AND METHODS

Patients

Physicians (T.F. and M.S.) collected BM samples from 437 Japanese gastric cancer patients who underwent surgery from 2001 to 2004 at the Central Hospital, National Cancer Center, Tokyo, Japan. Documented informed consent was obtained from all patients, and the study protocol was approved by the local ethics committee. The average age of the 293 male and 144 female patients was 61.9 years, with a range of 27–86 years (Table 1). Based on the Treaty for Japanese Gastric Cancer Association, 122 cases were classified as stage I, 109 as stage II, 101 as stage III, and 105 as stage IV.[28] Normal negative controls consisted of BM samples collected from 20 patients, with no malignancies (e.g., gallstone and hernia cases), between April 2000 to March 2003.

TABLE 1 *VIM* mRNA expression and clinicopathological factors

Factors	Positive (n = 178)		Negative (n = 259)		P value
	No.	%	No.	%	
Age (mean ± SD)	61.2 ± 11.7		62.4 ± 11.6		.31
Sex					
Male	111	62.4	182	70.3	.08
Female	67	37.6	77	29.7	
Histological grade					.29
Well, moderately	67	37.6	108	41.7	
Poorly, others	111	62.4	151	58.3	
Size	0.15				
<50 mm (small)	68	38.2	117	45.2	
>51 mm (large)	110	61.8	142	54.8	
Depth of tumor invasion					<.0001
m, sm	33	18.5	104	40.2	
mp, ss, se, si	145	71.5	155	59.8	
Lymph node metastasis					<.0001
Absent	38	21.4	117	45.2	
Present	140	78.6	142	54.8	
Lymphatic invasion					.001
Absent	59	33.2	126	48.7	
Present	119	66.8	133	51.3	
Venous invasion					.12
Absent	124	69.7	198	76.5	
Present	54	30.3	61	23.5	
Liver metastasis					.37
Absent	173	97.2	255	98.5	
Present	5	2.8	4	1.5	
Peritoneal dissemination					.92
Absent	161	90.5	235	90.7	
Present	17	9.5	24	9.3	
Distant metastasis					.19
Absent	168	94.4	251	96.9	
Present	10	5.6	8	3.1	
Recurrence					.87
Absent	173	97.2	251	96.9	
Present	5	2.8	8	3.1	
Stage					.01
I–II	81	45.5	150	57.9	
III–IV	97	54.5	109	42.1	

m tumor invasion of mucosa, *sm* submucosa, *mp* muscularis propria, *ss* subserosa, *se* penetration of serosa, *si* invasion of adjacent structures

BM Collection

Aspiration of BM was conducted under general anesthesia immediately before surgery as previously described.[26] The BM aspirate was obtained from the sternum using a BM aspiration needle. The first 1.0 ml of BM was discarded to avoid contamination by the skin. The second 1.0 ml of BM was added to 4.0 ml of Isogen-LS (Nippon Gene, Toyama, Japan), which was shaken vigorously and stored at −80°C until RNA extraction.

Total RNA Extraction and First-Strand cDNA Synthesis

Samples transferred from Tokyo to Beppu remained frozen while in transit. Total RNA was extracted from BM according to the manufacturer's protocol as described elsewhere.[29] The reverse transcriptase reaction (RT) was performed as previously described.[30] The first cDNA strand was synthesized from 2.7 μg of total RNA in 30 μl reaction mixtures containing 5 μl 5× RT buffer (Gibco BRL, Gaithersburg, MD), 200 μM dNTPs, 100 μM of a random hexadeoxynucleotide mixture, 50 units of RNasin (Promega, Madison, WI), 2 μl of 0.1 M dithiothreitol, and 100 units of Maloney leukemia virus RT (BRL). The mixture was incubated at 37°C for 60 min, heated to 95°C for 10 min, and then chilled on ice.

Cell Culture and Oxygen Deprivation

The human gastric cancer cell line NUGC3 was obtained from the Japanese Cancer Research Bank, Tokyo, Japan. The cell line was maintained in RPMI 1640 (Invitrogen Corp., Carlsbad, CA) supplemented with 10% fetal bovine serum (Equitec-Bio, Ingram, TX) and 100 units/ml penicillin G and streptomycin (Invitrogen). The cells were incubated in 5% CO_2 at 37°C and passaged every 3 days. Oxygen deprivation was carried out in an incubator with 1% O_2, 5% CO_2, and 94% N_2 at 37°C for 5 days.

Induction of EMT by TGF-β1

EMT induction by TGF-β1 was performed using a modification of methods described by Rees et al.[31] Cells were seeded into 6-well plates at 70% confluency and incubated in standard medium for 48 h. The cells were then incubated in serum-free medium supplemented with 5 μg/ml transferrin, 5 μg/ml insulin, 5×10^{-8} mol/l hydrocortisone, and 10 ng/ml endothelial growth factor (EGF) at 37°C in 5% CO_2 for 120 h with 0, 0.05, 0.5, or 5 ng/ml human TGF-β1 (R&D Systems, Inc., Minneapolis, MN). The culture medium was replaced daily.

Quantitative RT-PCR

The primer sequences used to amplify *VIM*, E-cadherin, slug, *ZEB1*, *SIP1*, twist, snail, N-cadherin, and *FN1* mRNA are shown in Supplemental Table 1. Glyceraldehyde-3-phosphate-dehydrogenase (*GAPDH*) was used as an internal control (Supplemental Table 1). Real-time monitoring of PCR reactions was performed using the LightCycler System (Roche Applied Science, Indianapolis, IN) and SYBR-Green I dye (Roche Diagnostics, Tokyo, Japan). Monitoring was performed according to the manufacturer's instructions, as previously described.[32] In brief, reactions were prepared on ice, containing 1 μl of cDNA, 1× DNA Master SYBR-Green I, 50 ng of primers, and 3 mM $MgCl_2$. The final volume was adjusted to 20 μl with water. After the reaction mixture was loaded into glass capillary tubes, quantitative RT-PCR was performed with the following cycling conditions: initial denaturation at 95°C for 10 min, followed by 40 cycles of 95°C for 10 s, annealing at 62°C for 10 s, and extension at 72°C for 10 s. After amplification, the amplicons were subjected to a temperature gradient from 67 to 95°C at 0.2°C/s, under continuous fluorescence monitoring, to produce a melting curve of the products.

Data Analysis for RT-PCR

After proportional baseline adjustment, the fit point method was employed to determine the cycle in which the log-linear signal was first distinguishable from the baseline. This cycle number was used as the crossing point value. A standard curve was produced by measuring the crossing point of each standard value and plotting it against the logarithmic value concentration. Concentrations of unknown samples were calculated by plotting their crossing points against the standard curve and dividing by *GAPDH* content.

Immunohistochemistry

Immunohistochemical studies for VIM and E-cadherin were performed on formalin-fixed, paraffin-embedded surgical sections obtained from gastric cancer patients. Tissue sections were deparaffinized, soaked in 0.01 M sodium citrate buffer, and boiled in a microwave for 5 min at 500 W to retrieve cell antigens. The primary mouse monoclonal antibodies against VIM (sc-6260 Santa Cruz Biotechnology) and E-cadherin (BD Biosciences) were used at a dilution of 1:50 and 1:100, respectively. Tissue sections were stained using an avidin-biotin-peroxidase protocol (LSAB+ system-HRP; DAKO, Kyoto, Japan) and counterstained with hematoxylin.

Immunocytochemistry

Cells were plated in poly-D-lysine coated 2-well culture slides (BD BioCoat Poly-D-Lysine 2-well culture slide, BD Biosciences) at a density of 1×10^5 cells/well. The cells were incubated in serum-free medium supplemented with 5 μg/ml transferrin, 5 μg/ml insulin, 5×10^{-8} mol/l hydrocortisone, and 10 ng/ml endothelial growth factor (EGF) at 37°C in 5% CO_2 for 120 h with 0, 0.05, or 5 ng/ml human TGF-β1. Culture medium was replaced daily. After treatment with TGF-β1, the cells were fixed in −20°C methanol for 10 min and stained with mouse monoclonal antibody against VIM (sc-6260 Santa Cruz Biotechnology) and E-cadherin (BD Biosciences). All sections were counterstained with hematoxylin.

Statistical Analysis

For continuous variables, data were expressed as the mean ± standard deviation. The relationship between *VIM* mRNA expression and clinicopathological factors was analyzed using a chi-square test and *t* test. Findings were considered significant when the *P* value was $< .05$. All tests were performed using JMP software (SAS Institute Inc., Cary, NC).

RESULTS

Clinicopathological Significance of VIM mRNA in BM of Gastric Cancer Patients

The mean expression level of *VIM* mRNA gradually increased concordantly with advanced clinical staging. Taking into consideration the clinical application of the current study, the 95% confidence interval was used to define the limits for the normal case cutoff values, according to the reference intervals of the Clinical and Laboratory Standards Institute.[33] Levels that were higher or lower than the cutoff values were defined as "positive" or "negative," respectively. The association between clinicopathological features and *VIM* mRNA expression is summarized in Table 1. In the *VIM*-positive group, the depth of tumor invasion, lymph node metastasis, and lymphatic invasion were significantly higher than in the *VIM*-negative group ($P < .0001$, $P < .0001$, and $P = .001$, respectively). In addition, the *VIM*-positive group had more advanced stage cases than the negative group ($P = .01$).

Immunohistochemistry of VIM and E-Cadherin Expression in Intratumoral Vessels of Gastric Cancer Patients

Expression of VIM protein in the primary lesions of resected gastric cancers was evaluated using immunohistochemistry. Cancer cells in the primary lesions did not stain with VIM antibody (Fig. 1a, b). However, some of the cells invading the intratumoral vessels were strongly positive for VIM (Fig. 1c, d), but were negative for E-cadherin. In contrast, the VIM-negative cells stained positively for E-cadherin (Fig. 1e, f).

TGF-β1 Alters Expression of VIM in Gastric Cancer Cells

We examined how TGF-β1 induction of EMT altered VIM expression in a gastric cancer cell line. NUGC3 cells were selected for EMT induction because of their low expression levels of *VIM* mRNA and VIM protein. VIM expression and morphological changes were evaluated using immunocytochemistry. Figure 2a, b show that cell

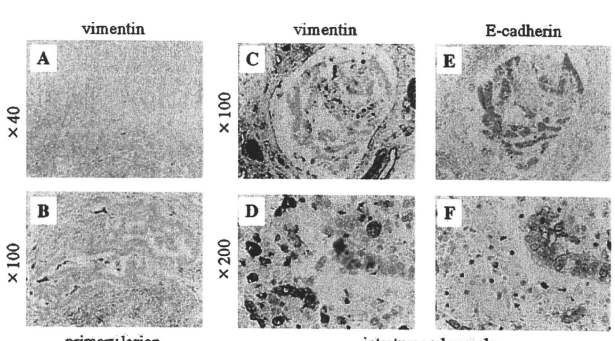

FIG. 1 Expression of VIM and E-cadherin proteins evaluated by immunohistochemistry of primary lesions in gastric cancer. **a, b** Cancer cells in the primary lesion did not express VIM. **c, d** Cells invading intratumoral vessels strongly expressed VIM. **e, f** VIM-positive cells in the intratumoral vessels were negative for E-cadherin. Conversely, VIM-negative cells were positive for E-cadherin

shape changed from round to fibroblastlike as VIM expression increased with the concentration of TGF-β1. In contrast, Fig. 2c, d shows that expression of E-cadherin was decreased by the addition of TGF-β1. The expression of *VIM* mRNA increased 5-fold after the addition of 5 ng/ml TGF-β1 (Fig. 2e). Levels of fibronectin and N-cadherin mRNA (mesenchymal markers) (data not shown) and slug mRNA (transcriptional repressor of E-cadherin) also rose as the concentration of TGF-β1 increased. Other transcriptional repressors of E-cadherin, such as snail, twist, SIP1, and ZEB1 mRNA, were not altered by TGF-β1 (data not shown). In contrast, the expression of E-cadherin mRNA decreased with increasing concentrations of TGF-β1 (Fig. 2e).

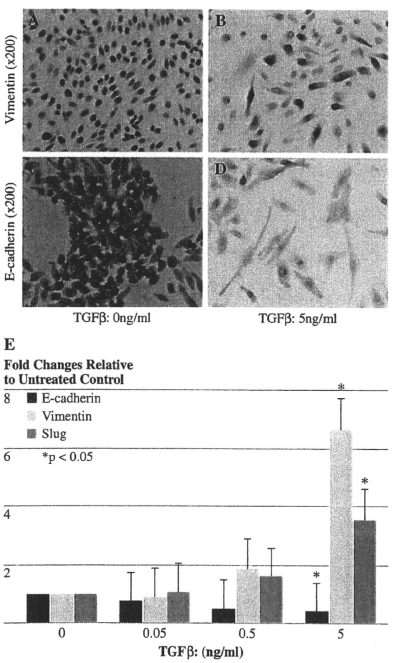

FIG. 2 Alteration of *VIM* expression in NUGC3 cells following addition of TGF-β1. **a, b** The shape of cells changed from round to fibroblast-like with increasing VIM expression after the addition of TGF-β1. **c, d** The expression of E-cadherin decreased after the addition of TGF-β1. **e** *VIM* and slug mRNA expression increased as the concentration of TGF-β1 increased, conversely, E-cadherin decreased. Data are expressed as the fold-change relative to the untreated control (TGF-β1: 0 ng/ml), * $P < .05$

Alteration of VIM Expression in Gastric Cancer Cells Under Hypoxic Conditions

After verifying VIM protein expression in NUGC3 cells under hypoxic conditions, VIM expression and morphological changes were evaluated by immunocytochemical analysis. Hypoxia stimulated an increase in VIM protein levels in NUGC3 cells and a change in shape from round to fibroblast-like (Fig. 3a, b). The loss of E-cadherin protein expression was observed with the alteration of cellular morphology (Fig. 3c, d). The expression of *VIM* mRNA under hypoxic conditions was significantly higher than that observed under normoxia, while E-cadherin mRNA decreased (Fig. 3e). Furthermore, slug mRNA also

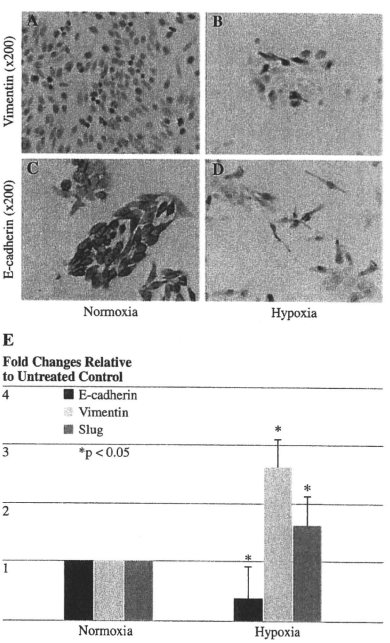

FIG. 3 Alteration of *VIM* expression in NUGC3 cells induced by hypoxia. **a, b** VIM expression in NUGC3 cells increased under hypoxic conditions with a change in shape from round to fibroblast-like. **c, d** E-cadherin expression decreased with an alteration of cellular morphology. **e** *VIM* and slug mRNA expression under hypoxic conditions was higher than under normoxia, conversely, E-cadherin decreased. Data are expressed as the fold-change relative to the untreated control (under normal conditions), * $P < .05$

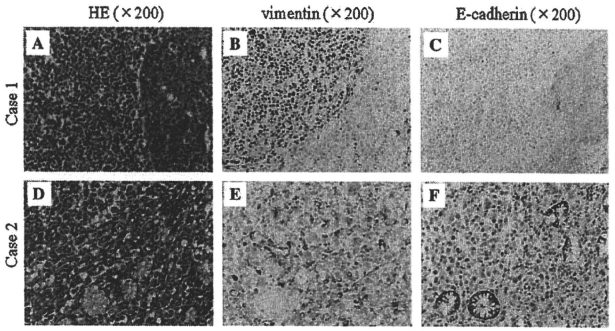

FIG. 4 Two cases of gastric cancer with rhabdoid features. In both cases (**a**, **b**, **c** Case 1; **d**, **e**, **f** Case 2), HE stained sections showed VIM-positive polygonal tumor cells had vesicular nuclei and abundant eosinophilic cytoplasm in an alveolar arrangement. VIM-positive tumor cells were negative for E-cadherin (**a**, **c** HE; **b**, **e** VIM; **c**, **f** E-cadherin: ×200)

increased under hypoxia as well as after addition of TGF-β1 (Fig. 3e).

Two Cases of Gastric Cancer with Rhabdoid Features

We examined the expression of VIM protein immunohistochemically in 30 poorly differentiated stomach adenocarcinomas. Two of these cases contained VIM-positive primary lesions. In both cases, hemotoxylin-eosin (HE) stained sections showed that the VIM-positive polygonal tumor cells had vesicular nuclei and abundant eosinophilic cytoplasm in an alveolar arrangement, as seen in malignant rhabdoid kidney tumors (Fig. 4a, b, d, e).[34] The VIM-positive tumor cells were E-cadherin-negative (Fig. 4c, f).

DISCUSSION

In advanced clinical cases of gastric cancer with invading tumor, lymph node metastasis, and lymphatic permeation, we found that the average expression level of *VIM* mRNA in BM was significantly higher than in the *VIM* negative group (Table 1). The current findings indicate that the abundant expression of *VIM* in BM primarily originates from cancer cells that have undergone mesenchymal transition in gastric cancer. Recent studies have shown that EMT plays a critical role in cancer progression and metastasis in epithelial malignancies other than gastric cancer.[9] VIM overexpression in cancer cells has become a focus of research efforts because it is a well-recognized representative mesenchymal marker.[35–37] In experimental models, EMT can be induced by TGF-β1 and hypoxia, which can produce metastatic phenotypes. However, there have been few studies of the induction of EMT by TGF-β1 and hypoxia in gastric cancer cells.[27,31] Our data show that the upregulation of VIM is induced by TGF-β1 and hypoxia with a concomitant alteration of cellular morphology (Figs. 2, 3). Importantly, among transcriptional repressors of E-cadherin, such as snail, twist, SIP1, and ZEB 1, we showed that in gastric cancer cells only slug mRNA rose along with the increasing concentration of TGF-β1 under hypoxic conditions. This finding may be supported by the previous report by Castro Alves et al.[38] that slug upregulation is associated with E-cadherin downregulation in diffuse and intestinal-type carcinoma.

With regard to the development of metastasis in solid cancer, isolated tumor cells detached from the primary site are able to survive against the hypoxic condition with the abundant expression of TGF-β1 in the circulating and disseminating systems, such as peripheral blood and bone marrow, by avoiding anoikis. Circulating gastric cancer cells in circulating system can overcome the deadly circumstance by the acquisition of a dynamic morphologic change, named EMT. In vitro, pancreatic cancer cells continuously exposed to TGF-β1 resist proliferation arrest and apoptosis following transfection of hypoxia inducible factor 1α (HIF-1α).[24,39] In breast cancer, Mehes et al.[40] reported that almost all breast cancer cells in the peripheral circulation were apoptotic. Therefore, our current findings imply that VIM-positive tumor cells can survive in the peripheral circulation and in BM and that VIM-positive cancer cells that invade intratumoral vessels must have undergone mesenchymal transition (Fig. 1).

To better understand the impact of the acquired mesenchymal phenotype on the progression of gastric cancer cases, we analyzed 2 well-defined cases. Carcinomas with rhabdoid features, which are extremely rare in gastrointestinal tract neoplasms and are highly malignant, are characterized by an aggressive clinical course.[41] Interestingly, 2 primary cases in

this study were VIM positive (Fig. 4). Therefore, aggressive VIM-positive rhabdoid gastric tumors have, like more typical gastric cancer that has metastasized to BM, mesenchymal features.

As for the origin of VIM-positive cells in BM, these are likely disseminated tumor cells. Immunochemistry showed that the cancer cells that invaded the intratumoral vessels were positive for VIM (Fig. 1). This finding in clinical samples suggests that circulating VIM-positive tumor cells not only survive in the peripheral circulation but can implant at metastatic sites. Here, we need to discuss the differences among ITC detection methods. The two main approaches for the detection of ITC are immunological assays using monoclonal antibodies and PCR-based molecular assays exploiting tissue-specific transcripts.[23] Immunocytochemical detection of epithelial or tumor-associated antigens is widely accepted.[42] We previously reported that RT-PCR assays targeting tumor-specific genes such as CEA and CK are useful to detect ITCs in various carcinomas.[29,30,43,44] However, in gastric cancer, there were no definitive data demonstrating that the detection of ITC was a useful prognostic marker (with either method) until our large-scale study.[26] We showed that > 50% of early gastric cancer cases expressed at least 1 ITC marker in PCR-based assays. Therefore, in the current study, we assume that not all detected ITCs but rather only a few that have undergone EMT, could give rise to metastasis or recurrence. On the other hand, one cannot neglect the enormous number of normal, VIM-positive cells in BM, such as precursors for fibroblasts, endothelial cells, macrophages, and lymphocytes that are associated with cancer progression. Recently, we described the importance of the synergistic relationship between tumor cells and BM-derived hematopoietic progenitor cells (HPCs) and endothelial progenitor cells (EPCs) in BM, as reported by Kaplan and Gao et al. previously.[25,26,45,46] In the current work, it is difficult to specify which cells might have expressed VIM protein. Therefore, it is possible that VIM expression originated from cancer cells and/or from normal cells in the BM.

In conclusion, we found that TGF-β1 and hypoxia upregulated VIM and inhibited E-cadherin in gastric cancer cells. The current data suggest that the abundant VIM expression, mainly from mesenchymal transited cancer cells in BM, might be associated with cancer progression and metastasis in gastric cancer.

ACKNOWLEDGMENT We thank T. Shimooka, K. Ogata, M. Kasagi, Y. Nakagawa, and T. Kawano for their technical assistance. This work was supported in part by the following grants and foundations: CREST, Japan Science and Technology Agency (JST); Japan Society for the Promotion of Science (JSPS) Grant-in-Aid for Scientific Research, grant numbers 20390360, 20591547, 20790960, 21591644, 21791295, 21791297, 215921014, and 21679006; NEDO (New Energy and Industrial Technology Development Organization) Technological Development for Chromosome Analysis.

REFERENCES

1. Beham A, Ratschek M, Zatloukal K, Schmid C, Denk H. Distribution of cytokeratins, vimentin and desmoplakins in normal renal tissue, renal cell carcinomas and oncocytoma as revealed by immunofluorescence microscopy. *Virchows Arch A Pathol Anat Histopathol.* 1992;421:209–15.
2. Raymond WA, Leong AS. Vimentin—a new prognostic parameter in breast carcinoma? *J Pathol.* 1989;158:107–14.
3. Upton MP, Hirohashi S, Tome Y, Miyazawa N, Suemasu K, Shimosato Y. Expression of vimentin in surgically resected adenocarcinomas and large cell carcinomas of lung. *Am J Surg Pathol.* 1986;10:560–7.
4. Miettinen M, Franssila K, Lehto VP, Paasivuo R, Virtanen I. Expression of intermediate filament proteins in thyroid gland and thyroid tumors. *Lab Invest.* 1984;50:262–70.
5. Utsunomiya T, Yao T, Masuda K, Tsuneyoshi M. Vimentin-positive adenocarcinomas of the stomach: co-expression of vimentin and cytokeratin. *Histopathology.* 1996;29:507–16.
6. Sommers CL, Heckford SE, Skerker JM, Worland P, Torri JA, Thompson EW, et al. Loss of epithelial markers and acquisition of vimentin expression in adriamycin- and vinblastine-resistant human breast cancer cell lines. *Cancer Res.* 1992;52:5190–7.
7. Sommers CL, Walker-Jones D, Heckford SE, Worland P, Valverius E, Clark R, et al. Vimentin rather than keratin expression in some hormone-independent breast cancer cell lines and in oncogene-transformed mammary epithelial cells. *Cancer Res.* 1989;49:4258–63.
8. Gilles C, Polette M, Piette J, Delvigne AC, Thompson EW, Foidart JM, et al. Vimentin expression in cervical carcinomas: association with invasive and migratory potential. *J Pathol.* 1996; 180:175–80.
9. Yang J, Weinberg RA. Epithelial-mesenchymal transition: at the crossroads of development and tumor metastasis. *Dev Cell.* 2008; 14:818–29.
10. Thiery JP. Epithelial–mesenchymal transitions in development and pathologies. *Curr Opin Cell Biol.* 2003;15:740–6.
11. Hay ED. Role of cell-matrix contacts in cell migration and epithelial-mesenchymal transformation. *Cell Differ Dev.* 1990;32: 367–75.
12. Batlle E, Sancho E, Franci C, Domínguez D, Monfar M, Baulida J, et al. The transcription factor snail is a repressor of E-cadherin gene expression in epithelial tumour cells. *Nat Cell Biol.* 2000;2: 84–9.
13. Comijn J, Berx G, Vermassen P, Verschueren K, van Grunsven L, Bruyneel E, et al. The two-handed E box binding zinc finger protein SIP1 downregulates E-cadherin and induces invasion. *Mol Cell.* 2001;7:1267–78.
14. Eger A, Aigner K, Sonderegger S, Dampier B, Oehler S, Schreiber M, et al. DeltaEF1 is a transcriptional repressor of E-cadherin and regulates epithelial plasticity in breast cancer cells. *Oncogene.* 2005;24:2375–85.
15. Hajra KM, Chen DY, Fearon ER. The SLUG zinc-finger protein represses E-cadherin in breast cancer. *Cancer Res.* 2002;62: 1613–8.
16. Yang J, Mani SA, Donaher JL, Ramaswamy S, Itzykson RA, Come C, et al. Twist, a master regulator of morphogenesis, plays an essential role in tumor metastasis. *Cell.* 2004;117:927–39.
17. Martin TA, Goyal A, Watkins G, Jiang WG. Expression of the transcription factors snail, slug, and twist and their clinical significance in human breast cancer. *Ann Surg Oncol.* 2005;12: 488–96.

18. Miyoshi A, Kitajima Y, Kido S, Shimonishi T, Matsuyama S, Kitahara K, et al. Snail accelerates cancer invasion by upregulating MMP expression and is associated with poor prognosis of hepatocellular carcinoma. *Br J Cancer.* 2005;92:252–8.
19. Uchikado Y, Natsugoe S, Okumura H, Setoyama T, Matsumoto M, Ishigami S, et al. Slug Expression in the E-cadherin preserved tumors is related to prognosis in patients with esophageal squamous cell carcinoma. *Clin Cancer Res.* 2005;11:1174–80.
20. Kim MA, Lee HS, Lee HE, Kim JH, Yang HK, Kim WH. Prognostic importance of epithelial-mesenchymal transition-related protein expression in gastric carcinoma. *Histopathology.* 2009;54:442–51.
21. Husemann Y, Geigl JB, Schubert F, Musiani P, Meyer M, Burghart E, et al. Systemic spread is an early step in breast cancer. *Cancer Cell.* 2008;13:58–68.
22. Pantel K, Brakenhoff RH. Dissecting the metastatic cascade. *Nat Rev Cancer.* 2004;4:448–56.
23. Pantel K, Brakenhoff RH, Brandt B. Detection, clinical relevance and specific biological properties of disseminating tumour cells. *Nat Rev Cancer.* 2008;8:329–40.
24. Gal A, Sjoblom T, Fedorova L, Imreh S, Beug H, Moustakas A. Sustained TGF beta exposure suppresses Smad and non-Smad signalling in mammary epithelial cells, leading to EMT and inhibition of growth arrest and apoptosis. *Oncogene.* 2008;27:1218–30.
25. Kaplan RN, Riba RD, Zacharoulis S, Bramley AH, Vincent L, Costa C, et al. VEGFR1-positive haematopoietic bone marrow progenitors initiate the pre-metastatic niche. *Nature.* 2005;438:820–7.
26. Mimori K, Fukagawa T, Kosaka Y, Kita Y, Ishikawa K, Etoh T, et al. Hematogenous metastasis in gastric cancer requires isolated tumor cells and expression of vascular endothelial growth factor receptor-1. *Clin Cancer Res.* 2008;14:2609–16.
27. Yang MH, Wu MZ, Chiou SH, Chen PM, Chang SY, Liu CJ, et al. Direct regulation of TWIST by HIF-1alpha promotes metastasis. *Nat Cell Biol.* 2008;10:295–305.
28. Maruyama K, Kaminishi M, Hayashi K, Isobe Y, Honda I, Katai H, et al. Gastric cancer treated in 1991 in Japan: data analysis of nationwide registry. *Gastric Cancer.* 2006;9:51–66.
29. Iinuma H, Okinaga K, Egami H, Mimori K, Hayashi N, Nishida K, et al. Usefulness and clinical significance of quantitative real-time RT-PCR to detect isolated tumor cells in the peripheral blood and tumor drainage blood of patients with colorectal cancer. *Int J Oncol.* 2006;28:297–306.
30. Mori M, Mimori K, Inoue H, Barnard GF, Tsuji K, Nanbara S, et al. Detection of cancer micrometastases in lymph nodes by reverse transcriptase-polymerase chain reaction. *Cancer Res.* 1995;55:3417–20.
31. Rees JR, Onwuegbusi BA, Save VE, Alderson D, Fitzgerald RC. In vivo and in vitro evidence for transforming growth factor-beta1-mediated epithelial to mesenchymal transition in esophageal adenocarcinoma. *Cancer Res.* 2006;66:9583–90.
32. Masuda TA, Inoue H, Sonoda H, Mine S, Yoshikawa Y, Nakayama K, et al. Clinical and biological significance of S-phase kinase-associated protein 2 (Skp2) gene expression in gastric carcinoma: modulation of malignant phenotype by Skp2 overexpression, possibly via p27 proteolysis. *Cancer Res.* 2002;62:3819–25.
33. Sasse EA. How to define and determine reference intervals in the clinical laboratory. NCCLS document C28-A2. Approved Guideline—Second Edition. National Committee for Clinical Laboratory Standards. 2000.
34. Weeks DA, Beckwith JB, Mierau GW, Luckey DW. Rhabdoid tumor of kidney. A report of 111 cases from the National Wilms' Tumor Study Pathology Center. *Am J Surg Pathol.* 1989;13:439–58.
35. Willipinski-Stapelfeldt B, Riethdorf S, Assmann V, Woelfle U, Rau T, Sauter G, et al. Changes in cytoskeletal protein composition indicative of an epithelial-mesenchymal transition in human micrometastatic and primary breast carcinoma cells. *Clin Cancer Res.* 2005;11:8006–14.
36. Hu L, Lau SH, Tzang CH, Wen JM, Wang W, Xie D, et al. Association of Vimentin overexpression and hepatocellular carcinoma metastasis. *Oncogene.* 2004;23:298–302.
37. McInroy L, Maatta A. Down-regulation of vimentin expression inhibits carcinoma cell migration and adhesion. *Biochem Biophys Res Commun.* 2007;360:109–14.
38. Castro Alves C, Rosivatz E, Schott C, Holloweck R, Becker I, Sarbia M, et al. Slug is overexpressed in gastric carcinomas and may act synergistically with SIP1 and Snail in the down-regulation of E-cadherin. *J Pathol.* 2007;211:507–15.
39. Akakura N, Kobayashi M, Horiuchi I, Suzuki A, Wang J, Chen J, et al. Constitutive expression of hypoxia-inducible factor-1alpha renders pancreatic cancer cells resistant to apoptosis induced by hypoxia and nutrient deprivation. *Cancer Res.* 2001;61:6548–54.
40. Mehes G, Witt A, Kubista E, Ambros PF. Circulating breast cancer cells are frequently apoptotic. *Am J Pathol.* 2001;159:17–20.
41. Amrikachi M, Ro JY, Ordonez NG, Ayala AG. Adenocarcinomas of the gastrointestinal tract with prominent rhabdoid features. *Ann Diagn Pathol.* 2002;6:357–63.
42. Braun S, Pantel K, Muller P, Janni W, Hepp F, Kentenich CR, et al. Cytokeratin-positive cells in the bone marrow and survival of patients with stage I, II, or III breast cancer. *N Engl J Med.* 2000;342:525–33.
43. Masuda TA, Kataoka A, Ohno S, Murakami S, Mimori K, Utsunomiya T, et al. Detection of occult cancer cells in peripheral blood and bone marrow by quantitative RT-PCR assay for cytokeratin-7 in breast cancer patients. *Int J Oncol.* 2005;26:721–30.
44. Mori M, Mimori K, Ueo H, Karimine N, Barnard GF, Sugimachi K, et al. Molecular detection of circulating solid carcinoma cells in the peripheral blood: the concept of early systemic disease. *Int J Cancer.* 1996;68:739–43.
45. Iwatsuki M, Fukagawa T, Mimori K, Nakanishi H, Ito S, Ishii H, et al. Bone marrow and peripheral blood expression of ID1 in human gastric carcinoma patients is a bona fide indicator of lymph node and peritoneal metastasis. *Br J Cancer.* 2009;100:1937–42.
46. Gao D, Nolan DJ, Mellick AS, Bambino K, McDonnell K, Mittal V. Endothelial progenitor cells control the angiogenic switch in mouse lung metastasis. *Science.* 2008;319:195–8.

Published OnlineFirst September 7, 2010; DOI:10.1158/1078-0432.CCR-10-0407

Clinical Cancer Research

Jumonji Domain Containing 1A Is a Novel Prognostic Marker for Colorectal Cancer: *In vivo* Identification from Hypoxic Tumor Cells

Mamoru Uemura, Hirofumi Yamamoto, Ichiro Takemasa, et al.

Clin Cancer Res 2010;16:4636-4646. Published OnlineFirst September 7, 2010.

Published OnlineFirst September 7, 2010; DOI:10.1158/1078-0432.CCR-10-0407

Imaging, Diagnosis, Prognosis

Clinical Cancer Research

Jumonji Domain Containing 1A Is a Novel Prognostic Marker for Colorectal Cancer: *In vivo* Identification from Hypoxic Tumor Cells

Mamoru Uemura[1], Hirofumi Yamamoto[1], Ichiro Takemasa[1], Koshi Mimori[3], Hideyuki Hemmi[1], Tsunekazu Mizushima[1], Masataka Ikeda[1], Mitsugu Sekimoto[1], Nariaki Matsuura[2], Yuichiro Doki[1], and Masaki Mori[1]

Abstract

Purpose: This study aimed to identify novel hypoxia-inducible and prognostic markers *in vivo* from hypoxic tumor cells.

Experimental Design: Using carbonic anhydrase 9 and CD34 as a guide for hypoxic tumor cells, laser capture microdissection was used to isolate colorectal cancer (CRC) liver metastases. The samples were analyzed by microarray analysis, in parallel with five CRC cell lines cultured under hypoxic conditions. To evaluate the prognostic impact of the expression of certain genes, samples from a total of 356 CRC patients were analyzed by microarray or quantitative reverse transcription-PCR. *In vitro* mechanistic studies and *in vivo* therapeutic experiments were also done about a histone H3 Lys^9 demethylase, Jumonji domain containing 1A (JMJD1A).

Results: Several candidate genes were identified by microarray analysis of liver metastases and culturing of CRC cells under hypoxic conditions. Among them, we found that JMJD1A was a novel independent prognostic factor for CRC ($P = 0.013$). *In vitro* assays revealed that loss of JMJD1A by small interfering RNA treatment was associated with a reduction of proliferative activity and decrease in invasion of CRC cell lines. Furthermore, treatment with an adenovirus system for antisense JMJD1A construct displayed prominent therapeutic effects when injected into established tumor xenografts of the CRC cell lines HCT116 and DLD1.

Conclusions: JMJD1A is a useful biomarker for hypoxic tumor cells and a prognostic marker that could be a promising therapeutic target against CRC. *Clin Cancer Res; 16(18); 4636–46. ©2010 AACR.*

Hypoxia is a characteristic of many solid tumors. Intratumoral hypoxia affects every major aspect of cancer biology, including cell invasion, metastasis, and determination of cell death (1). Intratumoral hypoxia and/or expression of the hypoxia-related endogenous proteins, vascular endothelial growth factor (VEGF), carbonic anhydrase 9 (CA9), hypoxia-inducible factor-1 (HIF-1), and glucose transporter 1 (GLUT1), are predictive of a poor prognosis in breast cancer (2), head and neck tumors (3), non–small cell lung cancer (4), cervical cancer (5), and colorectal cancer (CRC; ref. 6). There is also evidence that a hypoxia-related gene expression profile is associated with poor prognosis in human cancers (7). Taken together, these findings indicate that hypoxic conditions contribute to aggressive tumor behavior and to a more malignant phenotype.

Many molecules in the hypoxia-response pathway are good candidates for therapeutic targeting (8–10). The anti-VEGF antibody bevacizumab is used clinically for treatment of several human cancers (11), supporting that hypoxia-induced genes are clinically relevant therapeutic targets. Therefore, the identification of novel hypoxia-inducible genes holds great potential for the development of additional cancer therapies.

We aimed to identify, using microarray analysis, a novel prognostic factor and potential therapeutic target *in vivo* using hypoxic tumor cells from hepatic metastases of CRC. We found that Jumonji domain containing 1A (JMJD1A), a histone H3 Lys^9 demethylase, was a useful biomarker for hypoxic tumor cells and a poor prognosis of CRC. JMJD1A functions as a modulator of transcriptional activation of downstream target genes (12–14).

Authors' Affiliations: [1]Department of Surgery, Gastroenterological Surgery, Graduate School of Medicine and [2]Department of Pathology, School of Allied Health Science, Faculty of Medicine, Osaka University, Osaka, Japan; and [3]Department of Surgery and Molecular Oncology, Medical Institute of Bioregulation, Kyushu University, Beppu, Japan

Note: Supplementary data for this article are available at Clinical Cancer Research Online (http://clincancerres.aacrjournals.org/).

M. Uemura and H. Yamamoto contributed equally to this work.

Corresponding Author: Hirofumi Yamamoto, Department of Surgery, Gastroenterological Surgery, Graduate School of Medicine, Osaka University, 2-2 Yamada-oka, Suita City, Osaka, 565-0871, Japan. Phone: 81-6-6879-3251; Fax: 81-6-6879-3259; E-mail: hyamamoto@gesurg.med.osaka-u.ac.jp.

doi: 10.1158/1078-0432.CCR-10-0407

Published OnlineFirst September 7, 2010; DOI:10.1158/1078-0432.CCR-10-0407

Translational Relevance

Hypoxia is a characteristic feature of many solid tumors. Intratumoral hypoxia affects every major aspect of cancer biology. However, it is not easy to detect truly important hypoxia-inducible genes that are related to clinical cancer biology *in vitro* because cancer cells usually exist in chronically hypoxic conditions *in vivo* with complex interactions with several pathways. In this study, we showed that liver metastasis of colorectal cancer is a useful *in vivo* material to identify novel hypoxia-inducible and prognostic markers. This finding has great potential for extending our knowledge of hypoxia-related cancer biology and may provide guidance for developing novel cancer therapies. Furthermore, we have shown that a histone H3 Lys^9 demethylase, Jumonji domain containing 1A (JMJD1A), is a useful prognostic marker that can be a therapeutic target in colorectal cancer using the therapeutic xenograft model.

Because hypoxic tumor cells are likely to be resistant to cancer therapy, the present findings may provide clues for the development of a novel anticancer therapy.

Materials and Methods

Cell culture

HEK293 cells and human colon cancer cell lines HCT116, LoVo, DLD1, and HT29 were obtained from the American Type Culture Collection. The human colon cancer cell line KM12SM was a kind gift from Prof. T. Minamoto (Cancer Research Institute, Kanazawa, Japan). Cells were grown in DMEM supplemented with 10% fetal bovine serum, 100 units/mL penicillin, and 100 μg/mL streptomycin at 37°C in a humidified incubator with 5% CO_2. For culture under hypoxic conditions, cells were grown for up to 72 hours at 37°C in a continuously monitored atmosphere with a 1% O_2, 5% CO_2, and 94% N_2 gas mixture using a multigas incubator (model 9200, Wakenyaku Co.). Cells were cultured in normoxic conditions (21% O_2) as a control/reference.

Clinical samples

Hepatic metastases from CRC patients (n = 15) were consecutively collected exclusively during partial liver resection at Osaka University Hospital between 2000 and 2005. The samples of liver metastasis were embedded in OCT compound and frozen in liquid nitrogen within 10 to 15 minutes of resection. The samples were stored at −80°C until RNA extraction. For microarray analysis, we prospectively collected 214 primary CRC samples from consecutive patients who had curative operations in 2003 to 2006 from Osaka University Hospital and its nine associated hospitals. For quantitative reverse transcription-PCR (qRT-PCR), tumor samples were consecutively collected from a total of 142 CRC patients who had curative surgery from 1998 to 2002 at the Department of Surgery, Medical Institute of Bioregulation, Kyusyu University, and at its three associated institutes. The mean follow-up times were 44.0 ± 14.4 and 43.7 ± 33.5 months, respectively. The clinicopathologic features of patients from each institute, including gender, tumor location, extent of wall invasion, lymph node metastasis, histologic grade, clinical stage, and invasion to vein or lymphatic duct, are shown in Supplementary Table S1A and B.

In this study, none of the patients had preoperative chemotherapy or irradiation. After surgery, patients with stage III/IV tumors were basically treated with 5-fluorouracil–based chemotherapy. The surgical specimens were preserved in paraffin block and used for immunostaining of CD34 and JMJD1A. A piece of each primary CRC tissue sample was collected from the fresh specimens within 30 minutes after resection and stored in RNA Stabilization Reagent (RNAlater, Ambion, Inc.) at −80°C until RNA extraction. The RNA samples were kept at −80°C. For long-time storage, cDNA was routinely synthesized from RNA samples within 4 to 6 weeks after the operation and stored at −20°C. The Human Ethics Review Committee of Osaka University and Kyusyu University approved the use of the resected samples. REMARK criteria for tumor marker studies was used for the preparation of this article (15).

Immunohistochemistry and vessel count

Immunohistochemical analysis was done as described previously (16). Frozen sections (8 μm) were fixed in 4% paraformaldehyde for 5 minutes. The anti-CD34 mouse monoclonal antibody (1:500; Novocastra), anti-human CA9 goat polyclonal antibody (1:200; Santa Cruz Biotechnology), and anti-JMJD1A rabbit polyclonal antibody (1:100; Proteintech Group, Inc.) were incubated on the slides for 1 hour at room temperature. For negative controls, nonimmunized immunoglobulin G (Vector Laboratories) was used as a substitute for the primary antibody. Double staining of CD34 and CA9 was carried out as described previously (17). CA9 expression was scored as follows: 0, no staining; 1, weak staining; 2, moderate staining; and 3, strong staining. $CD34^+$ blood vessels were counted under a microscope at ×100 magnification. Ten visual fields were selected randomly in each portion of the metastatic CRC lesion, and the mean vessel counts per visual field were calculated. Vessel count was scored as follows: 0, no vessel staining; 1, 1 to 3 vessels; 2, 4 to 10 vessels; and 3, >10 vessels.

Western blot analysis

Western blot analysis was done as described previously (18). The membrane was incubated with the primary antibodies at the appropriate concentrations (1:800 for JMJD1A and 1:1,000 for actin) for 1 hour.

Published OnlineFirst September 7, 2010; DOI:10.1158/1078-0432.CCR-10-0407

Laser capture microdissection and microarray analysis

Laser capture microdissection (LCM) was done using the LM200 LCM system (Arcturus Engineering) as described previously (17). The quality check of total RNA and microarray analysis were carried out as described previously (19) using an oligonucleotide microarray covering 30,000 human probes (AceGene; DNA Chip Research, Inc. and Hitachi Software Engineering Co. Ltd.).

qRT-PCR

After reverse transcription, real-time monitoring of PCRs was done using the LightCycler system (Roche Applied Science) for quantification of mRNA expression (18). A housekeeping gene, porphobilinogen deaminase (PBGD), was used as an internal control (20). The PCR primers used in this study are listed in Supplementary Table S2.

Transfection of small interfering RNA

For small interfering RNA (siRNA) inhibition, double-stranded RNA duplexes targeting human *JMJD1A* (5′-AGAAGAAUUCAAGAGAUUCCGGAGG-3′/5′-CCUCCGGAAUCUCUUGAAUUCUUCU-3′) and negative control siRNA were purchased in a Stealth RNAi kit (Invitrogen). CRC cell lines were transfected with siRNA using Lipofectamine RNAiMAX (Invitrogen) according to the manufacturer's protocols.

Invasion assay

The invasion assay was done using Transwell cell culture chambers (BD Biosciences) as described previously (21). Briefly, 5×10^5 cells were seeded in triplicate on the Matrigel-coated membrane. After 48 hours, cells that had invaded the undersurface of the membrane were fixed with 100% methanol and stained with 1% toluidine blue. Four microscopic fields were randomly selected for cell counting.

Generation of an adenoviral antisense construct to JMJD1A

The entire coding sequence of human JMJD1A was amplified by RT-PCR with primers 5′-GGTACCGCCACCATGGTGCTCACGCTCGGAG-3′ and 5′-CTCGAGTTAAGGTTTGCCAAAACTGGATTCAC-3′ using mRNA prepared from KM12 cells. Adenoviral vectors containing

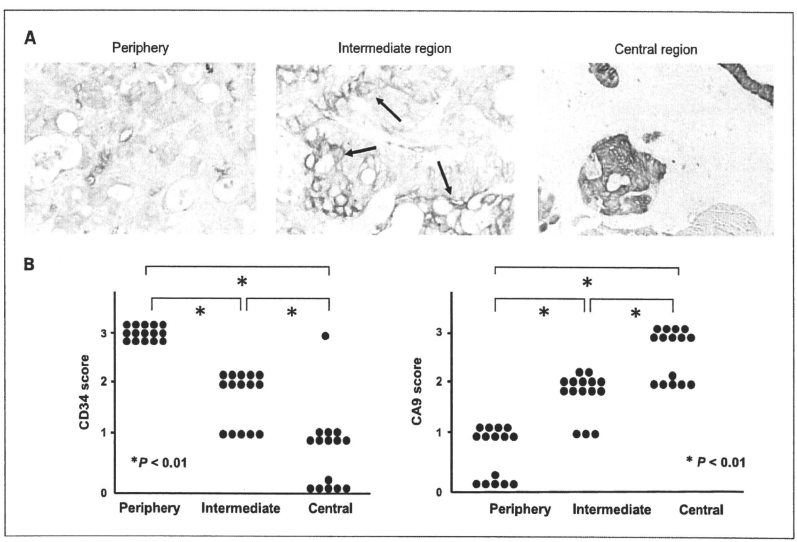

Fig. 1. Immunohistochemistry of CD34 and CA9 in liver metastasis. A, liver metastasis was double stained for CD34 as a vascular endothelial cell marker and CA9 as a hypoxic tumor cell marker. Tumor vessels (CD34; pink) decreased from the periphery to the central region. Conversely, CA9 expression in tumor cells (brown) increased from the periphery to the central region. Black arrows indicate that the intensity of CA9 staining was enhanced 80 μm from the tumor vessel. Magnification, ×400. B, scoring CD34 and CA9 staining. The CD34 score decreased significantly from the periphery to the central region ($P < 0.01$); conversely, the CA9 score increased significantly ($P < 0.01$). The details of each score are described in Materials and Methods. We then did LCM of $CD34^-CA9^+$ tumor cells around the central region and $CD34^+CA9^-$ tumor cells around the periphery of CRC liver metastasis.

Published OnlineFirst September 7, 2010; DOI:10.1158/1078-0432.CCR-10-0407

antisense JMJD1A were constructed using the AdEasy Adenoviral Vector System (Stratagene; ref. 21). Adenoviral recombination and preparation of infectious particles in HEK293 cells were described previously (22).

Treatment of established tumor xenografts by intratumoral injection of an adenoviral antisense construct to JMJD1A

Subcutaneous xenografts of the CRC cells DLD1 and HCT116 were established in nude mice ($n = 5$) by injection of 5×10^6 cells. After 1 week, when the tumor size reached 100 to 200 mm^3, Ad-Mock, adenoviral antisense (Ad-AS) construct to JMJD1A (1.0×10^9 plaque-forming units per injection), and NaCl solution were injected into tumors on days 7, 9, 11, and 13.

Statistical analysis

Statistical analysis was done using the StatView 5.0 program (Abacus Concepts, Inc.). The Kaplan-Meier method was used to examine disease-free survival, and the log-rank test was used to determine statistical significance. A Cox proportional hazard model was used to assess the risk ratio with simultaneous contributions from several covariates. Statistical analysis was done using the Student's *t* test or Fisher's exact test for categorical data and the Mann-Whitney *U* test for nonparametric data. Correlation significance was assessed using Pearson's correlation coefficient test. Values of $P < 0.05$ denoted a statistically significant difference.

Results

Immunohistochemistry of CD34 and CA9 in liver metastasis

To identify *in vivo* hypoxic tumor cells, we first did double staining of CD34 and CA9 using 15 hepatic metastases of CRC (Fig. 1A). The $CD34^+$ vascular endothelial cells (stained pink) significantly decreased from the periphery to the intermediate region to the central region of the metastasis. In contrast, CA9 expression in the tumor cells (stained brown) increased from the periphery to the central region (Fig. 1B). It was noteworthy that the intensity of CA9 staining became strong 80 μm from a tumor vessel in the intermediate region (Fig. 1A, middle), suggesting that CA9 is a sensitive marker for hypoxic tumor cells in hepatic metastasis of CRC.

LCM and microarray analysis

Using CA9 and CD34 as markers, $CD34^+CA9^-$ tumor cells in the periphery (Fig. 1A, left) and $CD34^-CA9^+$ tumor cells in the central region (Fig. 1A, right) were collected by LCM. After confirmation that high-quality RNA was derived from the tumor cells, 12 paired samples were subjected to microarray analysis.

The mean value of the fold induction in the central region relative to the periphery was calculated. Thirty genes with the greatest fold inductions are shown in Table 1, with the fold induction level ranging from 3.00 to 1.65. These 30 genes included well-known hypoxia-inducible genes, namely, egg-laying–defective nine homologue 3 (EGLN3), VEGF, endothelin-1 (EDN1), adrenomedullin (ADM), and peroxisome proliferator-activated receptor γ (PPARG). In addition, we found only a few reports that were related to hypoxia for prolyl-4-hydroxylase 1 (P4HA1), trefoil factor 3 (TFF3), endoplasmic reticulum oxidoreductin1-like (ERO1L), fatty acid binding protein (FABP4), and JMJD1A.

To investigate whether there were other novel hypoxia-inducible gene candidates, five colon cancer cell lines were subjected to microarray analysis after exposure to either hypoxic or normoxic conditions for 72 hours. We found that RNA levels were upregulated under hypoxic conditions in the genes that ranked 7th, 10th, 11th, 13th, 14th, 22nd, 23rd, 24th, and 29th in Table 1. The maximum induction of these genes was above 2.5-fold, which is comparable with the fold induction of known hypoxia-inducible genes (range, 1.2- to 8.3-fold).

Selection of novel biomarkers for malignant primary CRC

The well-known hypoxia-inducible genes VEGF, EDN1, EGLN3, TFF3, ADM, FABP1, and PPARG, listed in Table 1, were reported as poor prognostic factors for human malignancies (12, 23–32). To identify other genes that could serve as novel prognostic factors, we prospectively analyzed 214 CRC tissue samples using the same microarray chip; clinical data on disease recurrence were known for these samples. Our analysis indicated that JMJD1A (rank 9) and ADM (rank 21) were both significant prognostic markers for CRC. Although ADM was reported as a prognostic factor for ovarian cancer (30), JMJD1A has not been reported as a biomarker for human malignancies. Therefore, we subsequently focused on JMJD1A. A significant linear correlation of JMJD1A mRNA levels between microarray and qRT-PCR was observed ($P = 0.0004$; Supplementary Fig. S1A). Disease-free survival curves also showed that a high level of JMJD1A mRNA was a significant predictor of a shorter disease recurrence rate ($P = 0.0054$; Supplementary Fig. S1B). Supplementary Table S3 summarizes univariate and multivariate analyses for disease-free recurrence in the 214 CRC patients.

JMJD1A expression determined by qRT-PCR and immunohistochemistry

qRT-PCR analysis indicated that induced JMJD1A expression was 2.52-fold higher in the central region of liver metastasis compared with the periphery ($P = 0.0094$; Fig. 2A). Immunohistochemistry revealed that JMJD1A expression in the tumor cells (stained brown) increased from the periphery to the central region (Fig. 2B). Notably, the intensity of JMJD1A staining became strong 80 μm from a tumor vessel; this was also the case with CA9 staining. An approximately 3- to 6-fold induction of JMJD1A RNA was measured by qRT-PCR in the majority of CRC cell lines examined (Fig. 2C).

Published OnlineFirst September 7, 2010; DOI:10.1158/1078-0432.CCR-10-0407

Table 1. Microarray analysis of metastatic lesions in liver

Microarray data of liver metastasis				Representative gene symbol*	Gene ID	Accession
Rank	Mean fold	SD	Mann-Whitney *P*			
1	3	5.430236	0.41892	REG3A	5068	M84337
2	2.9	2.369342	0.02295	Unknown genes		BQ959777
3	2.68	1.069202	0.0003	EGLN3	112399	DQ975379
4	2.06	2.49874	0.45292	OLFM4	10562	NM_006418
5	2.04	1.009858	0.00042	VEGF	7422	AL136131
6	1.96	1.268504	0.00745	P4HA1	5033	NM_000917
7	1.91	1.447802	0.00324	RPGR	6103	NM_001034853
8	1.9	0.608637	0.01792	TFF3	7033	NM_003226
9	1.87	0.820366	0.00221	JMJD1A	55818	NM_018433
10	1.86	1.412287	0.15513	ACVR1	90	NM_001111067
11	1.84	1.227838	0.19141	RHOU	58480	NM_021205
12	1.81	1.428676	0.07419	EDN1	1906	NM_001955
13	1.79	1.173002	0.03123	OBSL1	23363	NM_015311
14	1.79	1.222501	0.0675	RGNEF	64283	NM_022448
15	1.78	0.78898	0.04157	HMBOX1	79618	NM_024567
16	1.78	1.274998	0.13091	FLJ21062	79846	NM_001039706
17	1.76	0.666219	0.00022	VEGF	7422	XM_052673
18	1.75	0.797286	0.14891	PSPH	5723	XM_028728
19	1.75	0.816036	0.02277	Unknown genes		AF189585
20	1.74	2.031618	0.62558	REG3A	5068	NM_002580
21	1.74	0.770142	0.00791	ADM	133	NM_001124
22	1.69	0.984528	0.00876	TARDBP	23435	NM_007375
23	1.68	0.965191	0.07556	SLCO1C1	53919	NM_017435
24	1.68	1.798507	0.84936	Unknown genes		AC009141
25	1.66	1.70151	0.18091	Unknown genes		AC005961
26	1.66	1.094456	0.52537	FABP1	2168	NM_001443
27	1.65	0.880628	0.1842	ERO1L	30001	NM_014584
28	1.65	0.885692	0.13719	SULF1	23213	NM_015170
29	1.65	0.618633	0.02434	ATP1B1	481	NM_001677
30	1.65	0.488769	0.00268	PPARG	5468	NM_015869

(*Continued on the following page*)

Survival survey

qRT-PCR was done using 142 independent CRC samples obtained from other institutes. High expression of JMJD1A RNA (n = 71, cutoff: median value; Supplementary Table S1B) was a significant prognostic factor with regard to cancer-related survival (P = 0.0108; Table 2). When analyzed with several clinicopathologic parameters that were statistically significant by univariate analysis, such as lymph node metastasis (P < 0.0001), lymphatic invasion (P < 0.0001), venous invasion (P = 0.0013), and depth of tumor invasion (P = 0.0008; Table 2), multivariate Cox regression analysis revealed that JMJD1A expression remained an independent prognostic factor (P = 0.0139; Table 2). As for the relationship between JMJD1A expression and each clinicopathologic characteristic, no significant difference was noted for age, gender, tumor location, and other factors (Supplementary Table S1B).

Effects of JMJD1A expression on growth and invasion of CRC cells

To assess the potential relevance of JMJD1A as a therapeutic target, *in vitro* knockdown experiments were done. Western blot analysis showed a significant reduction in the JMJD1A protein after siRNA treatment (Fig. 3A). A significant growth inhibition was observed in siRNA-treated HCT116 and DLD1 cell lines (P < 0.05 for each; Fig. 3B). Furthermore, invasion assays indicated that siRNA treatment significantly decreased the number of invaded cells of the two CRC cell lines when compared with control treatments (P < 0.05 for each; Fig. 3C).

Treatment of established tumor xenografts with an adenoviral construct of antisense JMJD1A

Similar to siRNA treatment, Ad-AS JMJD1A significantly decreased *in vitro* cell growth of the two CRC cells at a multiplicity of infection (MOI) of 100 (P < 0.05 for

Published OnlineFirst September 7, 2010; DOI:10.1158/1078-0432.CCR-10-0407

Table 1. Microarray analysis of metastatic lesions in liver (Cont'd)

Rank	Reported to be hypoxia-inducible genes		Reported as prognostic factor in cancers	Microarray data of five CRC cell lines (induction level under hypoxic condition)
	Well-known†	Limited number of reports		Median fold (range)
1				1.1 (0.86-1.82)
2				1.17 (0.4-1.91)
3	Yes		Yes	1.21 (0.95-5.44)
4				0.7 (1.08-1.22)
5	Yes		Yes	2.17 (0.85-4.04)
6		Yes		3.17 (2-7.42)
7			—	1.42 (0.4-2.95)
8		Yes	Yes	0.83 (0.69-3.5)
9		Yes		1.82 (1.02-8.33)
10				0.82 (0.41-2.9)
11				1.51 (0.16-3.25)
12	Yes		Yes	0.74 (0.28-1.22)
13				0.91 (0.7-3.93)
14				1.16 (0.34-2.74)
15				1.39 (0.62-1.86)
16				1.39 (1.02-2.26)
17	Yes		Yes	1.75 (1.25-2.39)
18				0.67 (0.62-1.28)
19				1.1 (0.49-1.45)
20				0.96 (0.72-1.32)
21	Yes		Yes‡	1.59 (0.75-1.9)
22				1.37 (0.8-2.6)
23				0.56 (0.17-2.7)
24				0.81 (0.44-6.3)
25				1.41 (0.98-1.54)
26		Yes	Yes	1.01 (0.87-1.18)
27		Yes		2.76 (1.69-8.15)
28				0.5 (0.33-1.03)
29				1.76 (1.55-5.05)
30	Yes		Yes	1.29 (1.02-1.92)

*Unknown genes contain genes such as ESTs and hypothetical proteins, whose function is unclear.
†Already well known as hypoxia-inducible gene; >50 publications related to hypoxia appear in the database of the National Library of Medicine (PubMed).
‡There is one reported as a prognostic factor in human cancer (ovarian cancer: $n = 60$, only in univariate analysis; ref. 35).

each; Fig. 4A). Similar results were obtained at MOI of 50 and 25 in both cells (data not shown). Treatment of established tumor xenografts, derived from the two cell lines, with intratumoral injection (four times) of Ad-AS JMJD1A significantly inhibited *in vivo* tumor growth when compared with the control groups ($P < 0.05$ for each; Fig. 4B).

Discussion

JMJD1A was initially identified in a testis cDNA library in 1991 (33), but its biological function has not yet been clarified. Studies gradually uncovered the roles of JMJD1A. JMJD1A is a histone H3 Lys^9 demethylase that causes transcriptional activation of certain downstream target genes (12–14), and it plays a role in embryonic stem cell differentiation (34) and spermatogenesis (13). Here, we report for the first time that JMJD1A could be an important prognostic factor for patients with CRC.

In a chronically hypoxic microenvironment, cancer cells undergo genetic and adaptive changes that allow them to become more clinically aggressive and to develop resistance to irradiation and chemotherapy (8, 9, 35). An efficient therapeutic strategy against those cell types is essential to overcome cancer, and we aimed to determine a novel molecular target that is induced under *in vivo* hypoxic conditions.

Published OnlineFirst September 7, 2010; DOI:10.1158/1078-0432.CCR-10-0407

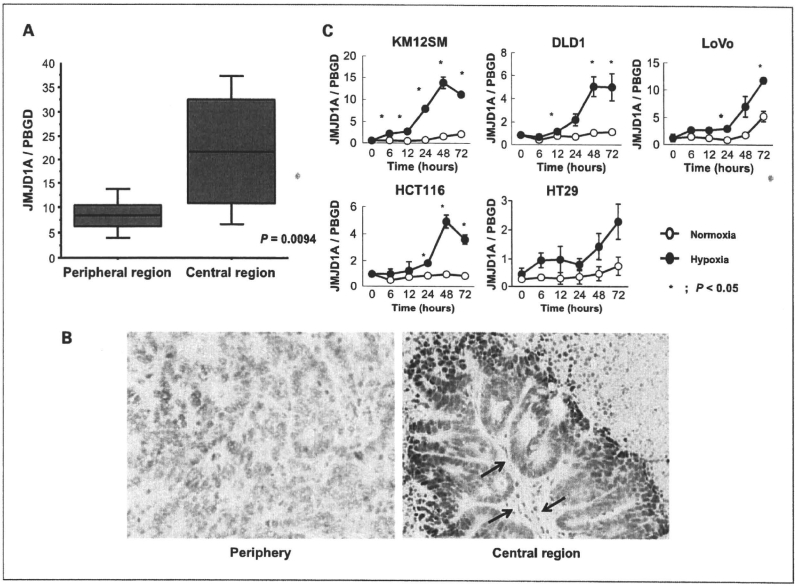

Fig. 2. Expression of JMJD1A in liver metastatic lesions. A, RT-PCR analysis indicated that JMJD1A expression had a 2.52-fold higher induction in the central region ($n = 12$; $P = 0.0094$). B, JMJD1A expression in tumor cells (brown) increased from the periphery to the central region. Black arrows indicate the tumor vessels. The intensity of JMJD1A staining was enhanced 80 μm from the tumor vessel. Magnification, ×200. C, quantitative analysis of JMJD1A gene expression in CRC cell lines under hypoxic conditions. In the majority of CRC cell lines, JMJD1A mRNA expression increased progressively under hypoxic conditions, with the maximum 3- to 6-fold induction at approximately 48 to 72 h. *, $P < 0.05$.

Table 2. Survival analysis of JMJD1A

Variable	Univariate analysis	Multivariate analysis	
	P	Relative risk (95% CI)	*P*
Lymph node metastasis (+/−)	<0.0001	6.282 (2.345-16.826)	0.003
Lymphatic invasion (yes/no)	<0.0001	3.535 (1.542-8.10)	0.0029
Duke's classification (CD/AB)	<0.0001		
Depth of invasion (ss~/~mp)	0.0008	1.522 (0.404-5.73)	0.5345
Venous invasion (yes/no)	0.0013	2.25 (1.041-4.86)	0.0392
JMJD1A (high/low)	0.0108	2.891 (1.235-6.43)	0.0139
Tumor site (rectum/colon)	0.264		
Gender (male/female)	0.2762		
Tumor dedifferentiation (moderate/poor/mucinous/well)	0.5574		
Age, y (≥68/<68)	0.9504		

Abbreviations: mp, muscularis propria; ss, subserosa.

Published OnlineFirst September 7, 2010; DOI:10.1158/1078-0432.CCR-10-0407

To find *in vivo* hypoxia-inducible genes, we studied liver metastases from CRC patients. The $CD34^+$ vascular architecture displayed a unique graded decline from the periphery to the central region (Fig. 1B); thus, it was easy to distinguish the region where hypoxic cells were present. We used CA9, which regulates cellular pH and allows cells to survive under hypoxic conditions, as a guide for hypoxic response. The distance from a vessel to the CA9 expression in cancer cells was 80 μm in head and neck tumors, leading to a tissue pO_2 of 1% (36). We also found that CA9 expression was strongly induced in tumor cells positioned approximately 60 to 100 μm from tumor vessels (Fig. 1A, middle), indicating that CA9 was a reliable biomarker for hypoxia in liver metastasis of CRC. In addition, the metastatic cells are thought to originate from a single proliferating cell (37, 38). The homogeneous cell population may be better suited for doing a reliable comparative gene expression study between cells supplied with an abundant flow of blood and those without. By contrast, primary cancer tissue consists of highly heterogeneous cells (39) and oxygen levels are typically heterogeneous within individual tumors (9).

To find novel hypoxia-inducible genes, the method of collecting liver metastasis samples is of particular importance. To avoid surgery-related hypoxia, we consecutively collected only patients who had partial liver resection, but not hepatic lobectomy or segmentectomy; the latter surgery usually requires ligation of the Glissonian branch to reveal a clear ischemic demarcation line on the surface of the liver. Moreover, we stored the liver tissue samples in OCT compound as soon as possible after removal by surgery, usually within 10 to 15 minutes. To assure that our collection method was effective enough to reduce surgery-associated hypoxia to a minimum, we did qRT-PCR before microarray analysis and examined whether well-known hypoxia-associated genes were upregulated in the central region of hepatic metastasis compared with the periphery region. We confirmed that the

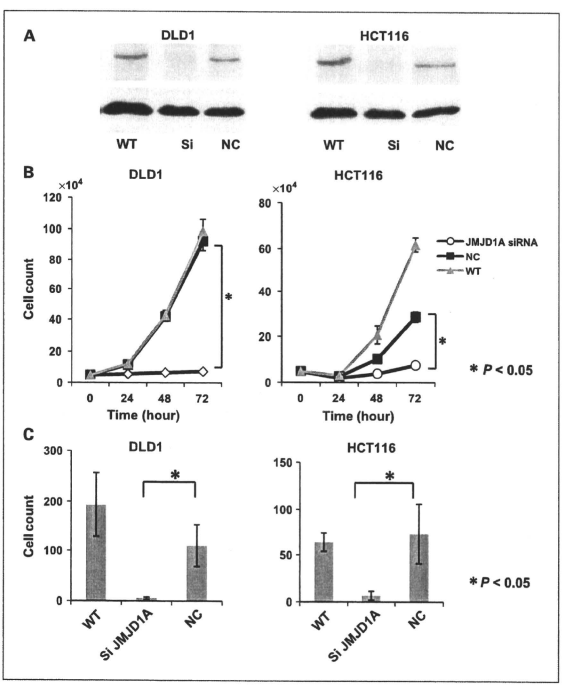

Fig. 3. *In vitro* assessment of JMJD1A expression after knockdown. A, cells were seeded at a density of 1.0×10^5 in six-well dishes in triplicate and counted 24, 48, and 72 h later using a hemocytometer. A significant reduction in JMJD1A by siRNA was noted by Western blotting in DLD1 and HCT116. Actin bands served as loading controls. WT, wild-type. B, cells were seeded at a density of 1.0×10^5 in six-well dishes. Treatment with JMJD1A siRNA displayed significant growth inhibition when compared with the negative control (NC) group in DLD1 and HCT116 ($P < 0.05$ for both). C, invasion assays showed a significant decrease in invaded cell number with treatment of JMJD1A siRNA in DLD1 and HCT116 ($P < 0.05$ for both).

Published OnlineFirst September 7, 2010; DOI:10.1158/1078-0432.CCR-10-0407

angiogenesis-related genes, such as angiopoietin2 (ANG2), VEGF, epidermal growth factor receptor (EGFR), fibroblast growth factor 2 (FGF2), and inducible nitric oxide synthase (iNOS), and the metabolism-related genes, such as GLUT1, GLUT3, lactate dehydrogenase A (LDHA), and phosphoglycerate kinase 1 (PGK1; refs. 1, 10, 40), showed 1.4- to 3.3-fold higher RNA in 12 paired samples (data not shown; primer sequences are shown in Supplementary Table S2). Microarray analysis successfully identified genes highly induced by hypoxia *in vivo*. VEGF ranked 5th among 30,000 human genes; 10 genes among the top 30 were well-known or relatively newly identified hypoxia-inducible genes (Table 1). We further identified several novel hypoxia-inducible gene candidates. The presence of many known hypoxia-related genes and prognostic factors in the list of the top 30 candidate genes is in good compliance with our initial concept that, *in vivo*, hypoxia-related genes should exert rather malignant properties. Because hypoxic stress is involved in cell death and survival, energy preservation, angiogenesis, pH regulation, and glucose metabolism, our data may shed some light on many aspects of cancer biology. After screening the top 30 genes based on a prospective clinical follow-up study in which the primary CRC tissues were analyzed with the same DNA chip, we focused on JMJD1A and concluded by qRT-PCR that JMJD1A is a novel independent prognostic factor for CRC (Table 2).

To assess the prognostic value of JMJD1A, it is important to see its relation to chemotherapy. When we analyzed disease-free survival between a group receiving chemotherapy and one that did not in a prospective series of 214 CRC patients (Supplementary Table S1A), we found that although a tendency was noted ($P = 0.059$), no statistical difference was observed between the two

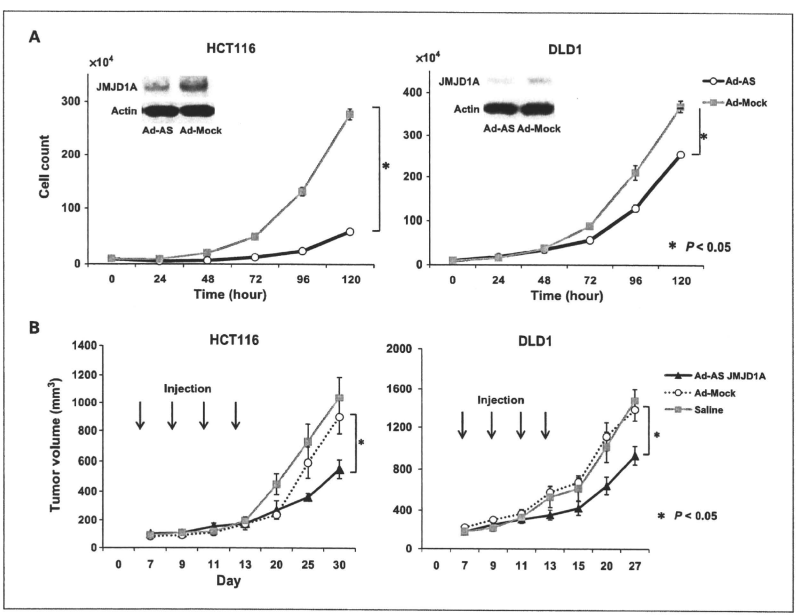

Fig. 4. Effects of Ad-AS JMJD1A on the growth of CRC cells. A, Ad-AS JMJD1A at MOI of 100 significantly inhibited tumor cell growth when compared with the Mock control in DLD1 and HCT116 ($P < 0.05$ for both). Western blot showed that Ad-AS JMJD1A at 100 MOI decreased JMJD1A protein expression at 48 h in DLD1 and HCT116. Actin bands served as loading controls. B, treatment of established tumor xenografts with intratumoral injection of Ad-AS JMJD1A. Subcutaneous xenografts of CRC cells (HCT116 and DLD1) were established in nude mice ($n = 5$ for each group) by injection of 5×10^6 cells. After day 7, Ad-Mock, Ad-AS JMJD1A (1.0×10^9 plaque-forming units per injection), and NaCl solution were injected into tumors and three more injections per tumor were applied on days 9, 11, and 13. Tumor size on day 30 was significantly smaller in the AS group when compared with the Mock control group in both cell types ($P < 0.05$ for both).

Published OnlineFirst September 7, 2010; DOI:10.1158/1078-0432.CCR-10-0407

groups (Supplementary Table S3). However, it was of interest that high expression of JMJD1A was significantly predictive of a poor prognosis in the group receiving chemotherapy ($P = 0.013$), but not in the group that did not receive chemotherapy (data not shown). The findings suggest that JMJD1A may lessen the efficacy of chemotherapy, which is consistent with the concept that hypoxia often makes tumor cells resistant to chemotherapy (8, 9, 35).

Recently, JMJD1A was shown for the first time to be upregulated by hypoxia via HIF-1 (41). Although Wellman et al. observed JMJD1A induction by hypoxia up to 24 hours, our data showed that the JMJD1A expression level continued to increase after 24 hours, reaching a maximum level of induction (3- to 6-fold) at 48 to 72 hours in CRC cell lines. In this regard, our gene list, generated from constitutive *in vivo* expression analysis, may reflect the chronic cellular responses to hypoxia. We also showed by immunohistochemistry that JMJD1A was a sensitive biomarker for *in situ* hypoxic cells (Fig. 2). The expression pattern was consistent with the report that hypoxic tumor cells are generally >100 μm away from functional blood vessels (42).

In vitro mechanistic studies showed that knockdown of JMJD1A reduced tumor cell growth and invasion. We also found that decreased growth effects from JMJD1A inhibition could be observed, irrespective of the VEGF level, in the colon cancer cells through treatment with siRNA against VEGF.[4] Furthermore, the therapeutic *in vivo* models using an adenovirus-mediated antisense strategy against JMJD1A showed that JMJD1A could be a promising therapeutic target in CRC. Epigenetic modifications can affect various characteristics of cancer cells, such as apoptosis, invasion, angiogenesis, and immune recognition (43); therefore, it is possible that JMJD1A has pleiotropic effects in CRC by restoring defective expression of certain genes. We also speculate that JMJD1A might be a universal prognostic factor in human carcinomas via histone modification because our prospective microarray analysis indicated that JMJD1A was associated with poor prognosis in gastric cancer and hepatocellular carcinoma (data not shown). Although many downstream targets should be clarified in the future, a recent study has shown that JMJD1A regulates the expression of ADM and growth and differentiation factor 15 (GDF15) by decreasing histone methylation of these promoters (44). The results are consistent with our findings that both JMJD1A and ADM are novel prognostic markers in CRC.

In conclusion, we showed that JMJD1A could be a sensitive biomarker for hypoxic tumor cells and a poor prognosis of CRC. Our data also suggest that JMJD1A may be a novel therapeutic target, especially against tumor cells in a hypoxic condition.

Disclosure of Potential Conflicts of Interest

There are no potential conflicts of interest in this study.

Acknowledgments

We thank Yurika Nakamura and Ken Konishi for their valuable technical support and Prof. T. Minamoto (Cancer Research Institute, Kanazawa, Japan) for providing the KM12SM colon cancer cell line.

Grant Support

3rd-term Comprehensive Strategy for Cancer Control from the Ministry of Health, Labour, and Welfare; Grant-in-Aid for Cancer Research from the Ministry of Education, Science, Sports, and Culture, Japan; and Sagawa Foundation for Promotion of Cancer Research.

The costs of publication of this article were defrayed in part by the payment of page charges. This article must therefore be hereby marked *advertisement* in accordance with 18 U.S.C. Section 1734 solely to indicate this fact.

Received 02/15/2010; revised 07/12/2010; accepted 07/13/2010; published OnlineFirst 09/07/2010.

[4] Unpublished observation.

References

1. Semenza GL. Hypoxia and cancer. Cancer Metastasis Rev 2007;26:223–4.
2. Colpaert C, Vermeulen P, van Beest P, et al. Intratumoral hypoxia resulting in the presence of a fibrotic focus is an independent predictor of early distant relapse in lymph node-negative breast cancer patients. Histopathology 2001;39:416–25.
3. Koukourakis MI, Giatromanolaki A, Sivridis E, et al. Hypoxia-regulated carbonic anhydrase-9 (CA9) relates to poor vascularization and resistance of squamous cell head and neck cancer to chemoradiotherapy. Clin Cancer Res 2001;7:3399–403.
4. Giatromanolaki A, Koukourakis MI, Sivridis E, et al. Expression of hypoxia-inducible carbonic anhydrase-9 relates to angiogenic pathways and independently to poor outcome in non-small cell lung cancer. Cancer Res 2001;61:7992–8.
5. Fyles A, Milosevic M, Hedley D, et al. Tumor hypoxia has independent predictor impact only in patients with node-negative cervix cancer. J Clin Oncol 2002;20:680–7.
6. Vaupel P, Mayer A. Hypoxia in cancer: significance and impact on clinical outcome. Cancer Metastasis Rev 2007;26:225–39.
7. Chi JT, Wang Z, Nuyten DS, et al. Gene expression programs in response to hypoxia: cell type specificity and prognostic significance in human cancers. PLoS Med 2006;3:e47.
8. Harris AL. Hypoxia—a key regulatory factor in tumour growth. Nat Rev Cancer 2002;2:38–47.
9. Kizaka-Kondoh S, Inoue M, Harada H, Hiraoka M. Tumor hypoxia: a target for selective cancer therapy. Cancer Sci 2003;94:1021–8.
10. Semenza GL. Targeting HIF-1 for cancer therapy. Nat Rev Cancer 2003;3:721–32.
11. Hurwitz H, Fehrenbacher L, Novotny W, et al. Bevacizumab plus irinotecan, fluorouracil, and leucovorin for metastatic colorectal cancer. N Engl J Med 2004;350:2335–42.
12. Arun C, London NJ, Hemingway DM. Prognostic significance of elevated endothelin-1 levels in patients with colorectal cancer. Int J Biol Markers 2004;19:32–7.
13. Okada Y, Scott G, Ray MK, Mishina Y, Zhang Y. Histone demethylase JHDM2A is critical for Tnp1 and Prm1 transcription and spermatogenesis. Nature 2007;450:119–23.
14. Yamane K, Toumazou C, Tsukada Y, et al. JHDM2A, a JmjC-containing H3K9 demethylase, facilitates transcription activation by androgen receptor. Cell 2006;125:483–95.

Published OnlineFirst September 7, 2010; DOI:10.1158/1078-0432.CCR-10-0407

15. McShane LM, Altman DG, Sauerbrei W, Taube SE, Gion M, Clark GM. REporting recommendations for tumor MARKer prognostic studies (REMARK). Nat Clin Pract Oncol 2005;2:416–22.
16. Hayashi N, Yamamoto H, Hiraoka N, et al. Differential expression of cyclooxygenase-2 (COX-2) in human bile duct epithelial cells and bile duct neoplasm. Hepatology 2001;34:638–50.
17. Ogawa M, Yamamoto H, Nagano H, et al. Hepatic expression of ANG2 RNA in metastatic colorectal cancer. Hepatology 2004;39: 528–39.
18. Yamamoto H, Kondo M, Nakamori S, et al. JTE-522, a cyclooxygenase-2 inhibitor, is an effective chemopreventive agent against rat experimental liver fibrosis. Gastroenterology 2003;125:556–71.
19. Takeno A, Takemasa I, Doki Y, et al. Integrative approach for differentially overexpressed genes in gastric cancer by combining large-scale gene expression profiling and network analysis. Br J Cancer 2008;99:1307–15.
20. Nagel S, Schmidt M, Thiede C, Huhn D, Neubauer A. Quantification of Bcr-Abl transcripts in chronic myelogenous leukemia (CML) using standardized, internally controlled, competitive differential PCR (CD-PCR). Nucleic Acids Res 1996;24:4102–3.
21. Hoshino H, Miyoshi N, Nagai K, et al. Epithelial-mesenchymal transition with expression of SNAI1-induced chemoresistance in colorectal cancer. Biochem Biophys Res Commun 2009;390: 1061–5.
22. Yasui M, Yamamoto H, Ngan CY, et al. Antisense to cyclin D1 inhibits vascular endothelial growth factor-stimulated growth of vascular endothelial cells: implication of tumor vascularization. Clin Cancer Res 2006;12:4720–9.
23. Ishigami SI, Arii S, Furutani M, et al. Predictive value of vascular endothelial growth factor (VEGF) in metastasis and prognosis of human colorectal cancer. Br J Cancer 1998;78:1379–84.
24. Arun C, DeCatris M, Hemingway DM, London NJ, O'Byrne KJ. Endothelin-1 is a novel prognostic factor in non-small cell lung cancer. Int J Biol Markers 2004;19:262–7.
25. Boldrini L, Gisfredi S, Ursino S, et al. Expression of endothelin-1 is related to poor prognosis in non-small cell lung carcinoma. Eur J Cancer 2005;41:2828–35.
26. Wulfing P, Diallo R, Kersting C, et al. Expression of endothelin-1, endothelin-A, endothelin-B receptor in human breast cancer and correlation with long-term follow-up. Clin Cancer Res 2003;9: 4125–31.
27. Couvelard A, Deschamps L, Rebours V, et al. Overexpression of the oxygen sensors PHD-1, PHD-2, PHD-3, and FIH is associated with tumor aggressiveness in pancreatic endocrine tumors. Clin Cancer Res 2008;14:6634–9.
28. Yamachika T, Werther JL, Bodian C, et al. Intestinal trefoil factor: a marker of poor prognosis in gastric carcinoma. Clin Cancer Res 2002;8:1092–9.
29. Dhar DK, Wang TC, Tabara H, et al. Expression of trefoil factor family members correlates with patient prognosis and neoangiogenesis. Clin Cancer Res 2005;11:6472–8.
30. Hata K, Takebayashi Y, Akiba S, et al. Expression of the adrenomedullin gene in epithelial ovarian cancer. Mol Hum Reprod 2000;6: 867–72.
31. Yamazaki T, Kanda T, Sakai Y, Hatakeyama K. Liver fatty acid-binding protein is a new prognostic factor for hepatic resection of colorectal cancer metastases. J Surg Oncol 1999;72:83–7.
32. Jiang Y, Zou L, Zhang C, et al. PPARγ and Wnt/β-catenin pathway in human breast cancer: expression pattern, molecular interaction and clinical/prognostic correlations. J Cancer Res Clin Oncol 2009;135: 1551–9.
33. Hoog C, Schalling M, Grunder-Brundell E, Daneholt B. Analysis of a murine male germ cell-specific transcript that encodes a putative zinc finger protein. Mol Reprod Dev 1991;30:173–81.
34. Loh YH, Zhang W, Chen X, George J, Ng HH. Jmjd1a and Jmjd2c histone H3 Lys 9 demethylases regulate self-renewal in embryonic stem cells. Genes Dev 2007;21:2545–57.
35. Brennan DJ, Jirstrom K, Kronblad A, et al. CA IX is an independent prognostic marker in premenopausal breast cancer patients with one to three positive lymph nodes and a putative marker of radiation resistance. Clin Cancer Res 2006;12:6421–31.
36. Beasley NJ, Wykoff CC, Watson PH, et al. Carbonic anhydrase IX, an endogenous hypoxia marker, expression in head and neck squamous cell carcinoma and its relationship to hypoxia, necrosis, and microvessel density. Cancer Res 2001;61:5262–7.
37. Fidler IJ. Selection of successive tumour lines for metastasis. Nat New Biol 1973;242:148–9.
38. Fidler IJ. The pathogenesis of cancer metastasis: the 'seed and soil' hypothesis revisited. Nat Rev Cancer 2003;3:453–8.
39. Korn WM, Yasutake T, Kuo WL, et al. Chromosome arm 20q gains and other genomic alterations in colorectal cancer metastatic to liver, as analyzed by comparative genomic hybridization and fluorescence *in situ* hybridization. Genes Chromosomes Cancer 1999;25:82–90.
40. Liao D, Johnson RS. Hypoxia: a key regulator of angiogenesis in cancer. Cancer Metastasis Rev 2007;26:281–90.
41. Wellmann S, Bettkober M, Zelmer A, et al. Hypoxia upregulates the histone demethylase JMJD1A via HIF-1. Biochem Biophys Res Commun 2008;372:892–7.
42. Helmlinger G, Yuan F, Dellian M, Jain RK. Interstitial pH and pO_2 gradients in solid tumors *in vivo*: high-resolution measurements reveal a lack of correlation. Nat Med 1997;3:177–82.
43. Sigalotti L, Fratta E, Coral S, et al. Epigenetic drugs as pleiotropic agents in cancer treatment: biomolecular aspects and clinical applications. J Cell Physiol 2007;212:330–44.
44. Krieg AJ, Rankin EB, Chan D, Razorenova O, Fernandez S, Giaccia AJ. Regulation of the histone demethylase JMJD1A by HIF-1α enhances hypoxic gene expression and tumor growth. Mol Cell Biol 2009;30: 344–53.

uicc
global cancer control

IJC
International Journal of Cancer

Loss of FBXW7, a cell cycle regulating gene, in colorectal cancer: clinical significance

Masaaki Iwatsuki[1,2], Koshi Mimori[1], Hideshi Ishii[1], Takehiko Yokobori[1], Yasushi Takatsuno[1], Tetsuya Sato[3], Hiroyuki Toh[3], Ichiro Onoyama[4], Keiichi I. Nakayama[4], Hideo Baba[2] and Masaki Mori[1]

[1] Department of Surgical Oncology, Medical Institute of Bioregulation, Kyushu University, Beppu, Japan
[2] Department of Gastroenterological Surgery, Graduate School of Medical Sciences, Kumamoto University, Kumamoto, Japan
[3] Division of Bioinformatics, Medical Institute of Bioregulation, Kyushu University, Fukuoka, Japan
[4] Department of Molecular and Cellular Biology, Division of Cell Biology, Medical Institute of Bioregulation, Kyushu University, Fukuoka, Japan

This study focused on a cell cycle regulatory gene, *FBXW7*, which ubiquitinates c-Myc and cyclin E and promotes exit from the cell cycle. We determined the expression level of *FBXW7* in colorectal cancer (CRC) cases, correlated those values with clinicopathologic features, and characterized the molecular mechanism of reduced expression of *FBXW7* in CRC cells *in vitro*. *FBXW7* mRNA and protein expression were evaluated in 93 CRC cases. Using CGH array, the copy number aberrations of the flanking region of *FBXW7* were evaluated in another 130 CRC specimens. *In vitro* analysis of *FBXW7* gene silencing in CRC cells was conducted. *FBXW7* mRNA expression was significantly lower in tumor tissues than the corresponding normal tissues. The low *FBXW7* expression group showed a significantly poorer prognosis than patients in the high expression group. A concordant relationship was observed between the incidence of *FBXW7* repression and the genetic alteration. The incidence of genetic alteration was associated with the stage of disease progression. *In vitro*, *FBXW7*-specific siRNA enhanced expression of c-MYC and cyclin E proteins and up-regulated cell proliferation. Genetic alterations in tumors led to the loss of *FBXW7* expression and increased cell proliferation. *FBXW7* expression provides a prognostic factor for patients with CRC.

Cancer Cell Biology

Normal cell growth and differentiation require appropriate regulation of the cell cycle. Deregulated cell cycle control is a fundamental aspect of cancer, resulting from mutation, deletion and transcriptional repression of genes such as pRB, and p53. Ubiquitin-mediated proteolysis is known to regulate the degradation of many proteins involved in the control of cell differentiation and growth.[1] Skp2 and FBXW7, F-box proteins containing components of the Skip1-Cull-F-box (SCF) ubiquitin ligase complexes, have been well characterized and shown to play important roles in degradation of proteins regulating cell cycle progression. Therefore, the altered expression of *FBXW7* is recognized to be one of the major causes of carcinogenesis or cancer development.[2–4] We have been focusing on expression of these cell cycle regulating genes in breast and gastric cancer.[5] In the current study, we examined FBXW7 which promotes the degradation of cyclin E, c-Myc, c-Jun and Notch and thereby negatively regulates these key oncoproteins.[6]

In an animal model, Onoyama *et al.* demonstrated conditional inactivation of Fbw7 in the T cell lineage of mice which later manifested thymic hyperplasia and eventually developed thymic lymphoma.[7] These results showed that FBXW7 plays an important role in malignant alterations of solid tumors. Thus far, there have been few studies regarding the clinicopathologic significance of *FBXW7* expression in human colorectal cancer (CRC).

In the present study, we examined copy number aberrations of *FBXW7* in a series of 130 CRC specimens using laser microdissection and a comprehensive genome hybridization (CGH) array. Then, we investigated *FBXW7* gene expression in another subset of 93 CRC samples with well-known clinicopathologic characteristics, including prognosis. The clinicopathologic significance of FBXW7 loss was validated biologically by CRC cell lines using siRNA interference.

Key words: FBXW7, colorectal cancer, c-Myc, cyclin E, CGH array
Additional Supporting Information may be found in the online version of this article.
Grant sponsor: CREST, Japan Science and Technology Agency (JST) and Japan Society for the Promotion of Science (JSPS) Grant-in-Aid for Scientific Research; **Grant numbers:** 17109013, 18659384, 18390367, 18590333, 18015039, 19591509, 19390336, 20390360, 20591547, 20790961, 20790960; **Grant sponsor:** The Ministry of Education, Culture, Sports, Science and Technology (MEXT) Grant-in-Aid for Scientific Research on Priority Areas; **Grant number:** 18015039; **Grant sponsor:** Third Term Comprehensive Ten-year Strategy for Cancer Control; **Grant number:** 16271201; **Grant sponsor:** New Energy and Industrial Technology Development Organization (NEDO) Technological Development for Chromosome Analysis
DOI: 10.1002/ijc.24879
History: Received 5 May 2009; Accepted 18 Aug 2009; Online 8 Sep 2009

Correspondence to: Masaki Mori, Department of Surgical Oncology, Medical Institute of Bioregulation, Kyushu University, 4546 Tsurumihara, Beppu 874-0838, Japan, Fax: +81-977-27-1651, E-mail: mmori@gesurg.med.osaka-u.ac.jp